Available online at www.sciencedirect.com
SCIENCE DIRECT®
PERGAMON
International Journal of Heat and Mass Transfer 46 (2003) 2527–2535
International Journal of HEAT and MASS TRANSFER
www.elsevier.com/locate/ijhmt

Critical quality prediction for saturated flow boiling of CO_2 in horizontal small diameter tubes

Rin Yun, Yongchan Kim *

Department of Mechanical Engineering, Korea University, Anam-dong, Sungbuk-ku, Seoul 136-701, South Korea

Received 13 September 2002; received in revised form 10 January 2003

Abstract

The dryout for flow boiling carbon dioxide (CO_2) in horizontal small diameter tubes is investigated through experiment and theoretical modeling. Tests are conducted in conditions where the saturation temperature is 0, 5, and 10 °C, heat flux is 7.2–48.1 kW/m^2 and mass flux is 500–3000 kg/m^2 s. The dryout phenomena of CO_2 are similar with those of water in many respects, while the effects of mass flux on dryout show differences among them. The dryout of CO_2 is predicted by a theoretical dryout model, which is developed and verified with steam–water data. Two entrainment mechanisms of interface deformation and bubble bursting are considered in the model and dryout is determined when the liquid film thickness is less than the critical liquid film thickness, the criteria film thickness of dryout. The present model well predicts the experimental critical qualities except when mass flux is relatively high, at which the deposition of liquid droplet on the liquid film and the occurrence of dryout patches become very significant.

Keywords: Dryout; CO_2; Evaporation; CHF model

1. Introduction

Due to environmental concerns on the global warming of hydrofluorocarbon (HFC) refrigerants, many studies have been performed on the applications of carbon dioxide (CO_2) in mobile air-conditioners, water heaters, and heat pumps [1]. CO_2 is environmentally safe and has favorable thermodynamic properties as a refrigerant. However, it was found that the transcritical cycle of CO_2 might yield a lower performance in comfort cooling application than the typical unitary equipment using conventional refrigerants such as R22, R134a, and R410A [1]. It is essential to improve the efficiency of each component in the CO_2 system to overcome this disadvantage. Especially, a novel shape of heat exchangers satisfying high efficiency, safety, and compactness need to be developed. Microchannel tubes have been considered as a replacement of the conventional fin-tube heat exchanger in the CO_2 transcritical cycle due to higher efficiency, lower pressure drop, less heat exchanger core volume, and lower refrigerant charge [2].

The critical heat flux condition (CHF) for internal flow boiling is used to describe the conditions at which the wall temperature increases and the heat transfer coefficient drops sharply due to a change in the heat transfer mechanism. For saturated conditions at moderate to high qualities in the tube of an evaporator, the CHF most often corresponds to dryout of the liquid film on the tube wall, which is usually referred to simply as dryout. The dryout phenomenon of CO_2 occurs at a normal saturation temperature in the transcritical cycle. The dryout of CO_2 is attributed to its thermodynamic properties, which tend to increase liquid droplet entrainment [3]. In addition, dryout conditions are dependent on mass flux, heat flux, and saturation temperature. Since the dryout significantly lowers the performance of heat exchangers, both the selection of appropriate operating conditions and the optimal design of heat exchangers are required to avoid dryout. However, so far, the occurrence of dryout for flow boiling of CO_2 with a

* Corresponding author. Tel.: +82-2-3290-3366; fax: +82-2-921-5439.
E-mail address: yongckim@korea.ac.kr (Y. Kim).

0017-9310/03/$ - see front matter
doi:10.1016/S0017-9310(03)00036-X

Nomenclature

C	concentration in the vapor core (kg/m^3)
D	tube inner diameter (m)
d	deposition rate (kg/m^2 s)
e	entrainment rate (kg/m^2 s)
g	acceleration of gravity (m/s^2)
h_{fg}	latent heat of vaporization (J/kg)
K	correction factor
k	deposition mass transfer coefficient (m/s)
G	mass flux (kg/m^2 s)
Pr	Prandtl number
q	heat flux (W/m^2)
Re	film Reynolds number
U_g	superficial gas velocity (m/s)
x	vapor quality
w	mass flow rate (kg/s)
Z	channel length (m)

Greek symbols

Γ	mass flow rate per unit periphery of tube (kg/ms)
δ	liquid film thickness (m)
θ	contact angle between the liquid–vapor interface and solid surface (°)
μ	dynamic viscosity coefficient (Ns/m^2)
v	kinematic viscosity (m^2/s)
ρ	fluid density (kg/m^3)
σ	surface tension (N/m)
τ	shear stress (N/m^2)

Subscripts

bo	dryout
c	critical
d	droplet
e	equilibrium
en	entrainment
exp	experiment
f	fluids, liquid phase
g	gas phase
hor	horizontal
i	interface
in	inlet
lf	liquid film
lfc	liquid film, critical
lg	interface between liquid and gas
max	maximum
min	minimum
out	outlet
pre	prediction
sg	interface between solid and gas
ver	vertical

variation of operating conditions in small diameter tubes has not been fully investigated.

Pettersen et al. [2] and Hihara and Tanaka [4] experimentally investigated the dryout of CO_2. Pettersen et al. [2] tested microchannel tubes with a hydraulic diameter of 0.79 mm. They found that dryout was dependent on saturation temperature, mass flux, and heat flux. Hihara and Tanaka [4] presented the evaporation heat transfer coefficient of CO_2 in a 1.0 mm diameter tube. Although a rapid drop of heat transfer coefficient was observed in their data, the dryout of CO_2 was not discussed in detail and test conditions were also very limited. Only few theoretical analysis of dryout for CO_2 in small diameter tubes can be found in open literature. Neksa and Pettersen [5] predicted the critical quality by using the Ahamd method. Ahmad [6], Katto and Ohno [7], Pioro et al. [8] used similarity factors in the prediction of CHF for non-water fluids. Basically, the similarity factor was to convert non-water fluid conditions to equivalent steam–water conditions to attain the applicability of the correlations developed for the steam–water evaporation.

The objectives of this study are to explain dryout characteristics observed in the experiments and to develop an analytical prediction model of critical quality during the evaporation process of CO_2 in small diameter tubes. The effects of mass flux and heat flux on dryout are experimentally investigated through a wide spectrum of test conditions. Besides, CHF and critical quality are predicted by applying an appropriate analytic flow model with similarity factors. The analytic model provides explanations for liquid droplet entrainment and the effects of surface tension during the dryout of CO_2.

2. Experiments

Fig. 1 shows a schematic of the experimental setup. The test facility consists of a magnetic gear pump, a mass flow meter, a preheater, a test section, and a heat exchanger. The pump circulates CO_2, and the preheater is used to adjust the inlet vapor quality of the test section. The refrigerant having a high quality at the exit of the test section is completely condensed and subcooled by the condenser. Applying a direct current heating method provides heat flux to the test section.

The test sections used in this study are horizontal smooth tubes with inner diameters (ID) of 2.0 and 0.98 mm, which are made of stainless steel. The outside diameter is 3.2 and 1.6 mm and the heated length is 1200

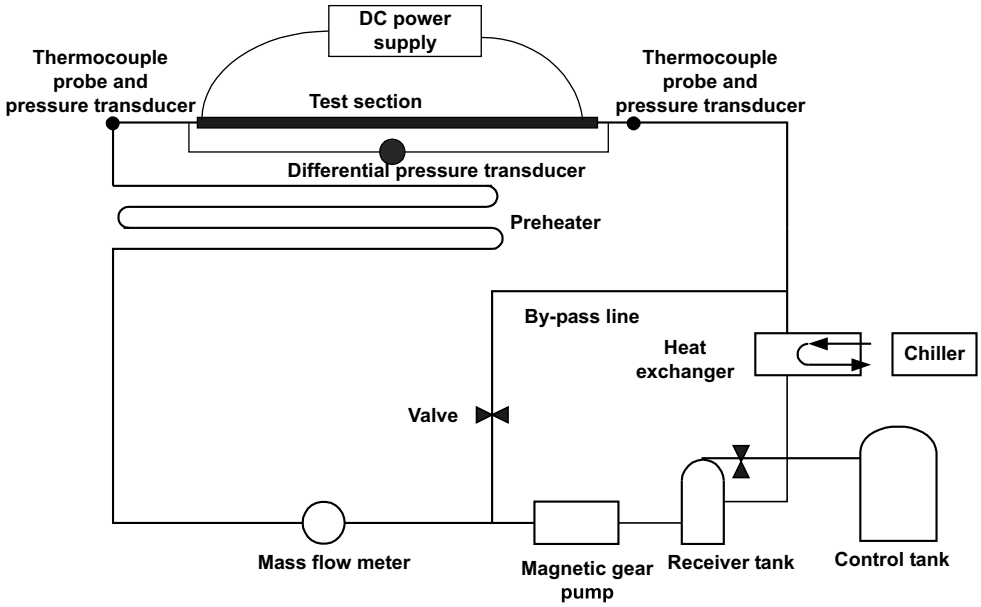

Fig. 1. Schematic of the experimental setup.

and 400 mm for the 2.0 and 0.98 mm ID tube, respectively. Thermocouples are placed at the top and the bottom of each location, which is equally located along the test section with an interval of 200 mm for the 2.0 mm ID tube and 70 mm for the 0.98 mm ID tube. The thermocouple junctions are electrically insulated from the tube using a very thin Teflon tape.

The refrigerant flow rate is measured using a Coriolis effect flow meter with an uncertainty of a ±0.2% reading. Wall temperatures of the test section are measured by T-type thermocouples with a calibrated accuracy of ±0.1 °C. The refrigerant temperatures at each thermocouple junction are linearly interpolated from the measured data at the inlet and outlet of the test section using thermocouple probes with an uncertainty of ±0.1 °C. The power inputs to the preheater and the test section are monitored using a watt transducer with an uncertainty of ±0.2% on full scale. Heat loss to the ambient is within 5% of the electric heat input, and it is taken into account in the experiments. The experimental uncertainty of quality is approximately ±0.02 at all test conditions.

For the 0.98 mm ID tube, the tests are conducted at heat fluxes of 20, 30, and 40 kW/m^2, mass fluxes of 1000, 1500, and 2000 kg/m^2 s, and saturation temperatures of 0, 5, and 10 °C. For the 2.0 mm ID tube, the test conditions for heat flux and saturation temperature remain the same as those for the 0.98 mm ID tube, but mass flux is varied from 500 to 3000 kg/m^2 s with an interval of 500 kg/m^2 s. Since the heat transfer characteristics are measured during the evaporation process, the inlet temperature of the test section is equal to the saturation temperature.

For saturated conditions at moderate to high qualities, the flow is almost invariably in annular flow and dryout patches occur in the liquid film due to liquid droplet entrainment into the vapor core and vaporization. These patches are expanded or rewetted according to the external conditions, and finally the liquid film dries out. Once dryout occurs, the flow exists in mist flow and the wall temperature rises, resulting a rapid decrease in the heat transfer coefficient. In this experiments, critical quality, which corresponds to dryout, is determined when the wall superheat rapidly increases.

3. Development of an analytical model for critical quality prediction

3.1. Annular flow model with liquid entrainment

In this study, the critical quality during flow boiling of CO_2 is determined by using an analytical approach based on the correlations for flow boiling of steam–water. The saturation pressure significantly affects the flow pattern in the boiling process, which plays an important role in dryout phenomenon [9]. The test data and flow patterns for the dryout of steam–water at a high pressure can be used in the prediction of critical quality for CO_2, because the transcritical CO_2 cycle operates at high saturation pressures. However, the similarities of thermophysical properties between CO_2

and steam–water mixture have to be satisfied before applying the data for flow boiling of water to CO_2. When the test conditions of CO_2 such as pressure, heat flux, and tube diameter are converted to equivalent steam–water conditions as described by Pioro et al. [8], the viscosity of CO_2 shows a similar value with that of equivalent steam–water. The surface tension of CO_2 is 50% lower than that of equivalent steam–water. However, introducing the non-dimensional parameters of liquid drop entrainment factor, $\tau_i\delta/\sigma$ [10], and critical liquid film thickness [11,12] can successfully compensate the difference of surface tension, satisfying the similarity between CO_2 and steam–water.

The critical quality of CO_2 is calculated in the following procedure: (1) convert operating conditions for CO_2 to equivalent steam–water conditions using similarity factors [8], (2) apply the annular flow model with the converted conditions such as heat flux, mass flux and saturation pressure, and (3) determine the critical quality by comparing the calculated liquid film thickness of the model with the critical liquid film thickness.

Generally, two methods have been used to predict critical heat flux and critical quality. One method is an estimation of liquid film flow rate with respect to tube length as given in [13–15],

$$\frac{dw_{lf}}{dZ} = \pi D\left(d - e - \frac{q}{h_{fg}}\right) \tag{1}$$

where d is the deposition rate, e is the entrainment rate, and w_{lf} is the liquid film mass flow rate. The other method is an application of constitutional equations to vapor core, liquid film, and interface between vapor and liquid [16].

In this study, the liquid film thickness, the film flow rate, and the pressure drop are calculated by applying the second method with an assumption of annular flow pattern. Liquid film thickness is determined by solving the governing equations suggested by Carey [17], and entrainment models shown in Eqs. (2)–(5) are used to calculate liquid film thickness. Liquid droplet entrainment is calculated by considering two mechanisms of droplet formation, which was also utilized in Celata et al.'s CHF model [13]. One mechanism is that the entrainment is resulted from extreme deformation of wavy interface between liquid film and vapor core [18]. Eq. (2) [15] describes the wave deformation mechanism of entrainment. The other is that the bubble bursting occurred near interface yields liquid droplet entrainment in vapor core. Eqs. (3) [12] and (4) [19] include the entrainment due to bubble bursting. Deposition mass transfer coefficient, k in Eq. (5), follows the correlation suggested by Hewitt and Goven [15].

$$e_W/G_g = 5.75\times10^{-5}\left[(G_{lf}-G_{lfc})^2\frac{D\rho_f}{\sigma\rho_g^2}\right]^{0.316} \tag{2}$$

$$e_B = 5.3\times10^{-15}I^{0.5}q^{2.5} \quad \text{for } q < 500\ \text{kW/m}^2,\ \Gamma_{in} < 1.0\ \text{kg/ms} \tag{3}$$

$$\frac{e_B}{q/h_{fg}} = 4.77\times10^2\left[\frac{(q/h_{fg})^2\delta}{\sigma\rho_g}\right]^{0.75} \quad \text{for } q \geqslant 500\ \text{kW/m}^2,\ \Gamma_{in} < 1.0\ \text{kg/ms} \tag{4}$$

$$(e_W + e_B) = kC_e \tag{5}$$

To decide which value of liquid film thickness results in permanent dryout, critical liquid film thickness theoretically developed by Fujita and Ueda [11,12] is used. According to Fujita and Ueda [11,12], distortion of liquid film, which is promoted by the surface tension difference set up in the film, forms a thin film region and a dryout patch occurs at the thin film region. Thickness of this thin film, which is called critical liquid film thickness, is calculated with Eqs. (6) and (7). If the liquid film thickness calculated by the present model is less than δ_c, dryout occurs.

$$\delta_c = 0.35\delta/Pr^{1/4} \tag{6}$$

$$\delta = \left(\frac{3}{4}\frac{\nu^2}{g}Re\right)^{1/3} \qquad Re = 4\Gamma_{f,out}/\mu \tag{7}$$

The value of δ_c is determined when the flow pattern starts to change into annular flow, namely U_g^* in Eq. (8) [15] where it is equal to 1. In deriving Eq. (6), derivative equations must be solved in thin liquid film. So to get stable results for these equations, steady liquid film is necessary. When U_g^* is equal to 1, relatively uniform and steady liquid film is formed.

$$U_g^* = \frac{U_g\rho_g^{1/2}}{\sqrt{(gD(\rho_f-\rho_g))}} \tag{8}$$

3.2. Validation of the annular flow model

To assure the validity of the present model, verification is made in two aspects. First, the liquid film flow rate and entrainment flow rate are compared with available experimental data [20] as shown in Table 1. This comparison gives assurance of using two separate mechanisms in explaining liquid droplet entrainment as indicated in Eq. (5). Second, critical qualities are compared with 560 dryout data of steam–water [21]. Fig. 2 shows the comparison between dryout data [21] for flow of boiling water and that predicted from the present model. Among the total data, 92% lies within ±0.3 of $|x_{bo,exp} - x_{bo,pre}|$. This comparison verifies the present annular flow model and criteria of critical film thickness proposed in Eqs. (6) and (7).

Table 1
Prediction of liquid entrainment for steam–water flow in a vertical tube with heat addition

Run no.	Mass flux ($kg/m^2 s$) $\times 10^3$	Water flow rate (kg/s) $\times 10^{-2}$	Power (W) $\times 10^5$	Subcooling (J/kg) $\times 10^5$	Heat flux (W/m^2) $\times 10^5$	Outlet steam quality (%)	Film flow rate (kg/s) $\times 10^{-2}$			Entrainment rate (kg/s) $\times 10^{-2}$		
							Exp.[a]	Model	Deviation (%)[b]	Exp.[a]	Model	Deviation (%)[b]
1	1.36	16.99	1.45	1.674	9.94	44.9	0.832	0.75	−9.8	8.51	8.51	0
2	1.36	16.99	1.315	1.674	9.84	39.8	2.215	1.03	−53.5	7.97	9.01	13.05
3	1.36	16.95	1.199	1.534	9.78	36.5	2.552	1.30	−49.1	8.18	9.3	13.69
4	1.36	16.98	1.079	1.489	9.91	32.2	3.085	1.78	−42.3	8.43	9.54	13.17
5	1.36	16.91	0.958	1.651	9.87	26.5	3.820	2.79	−26.9	8.6	9.47	10.12
6	1.36	17.01	0.832	1.651	9.81	21.5	4.380	4.29	−2.05	8.95	8.81	−1.56
7	2.04	25.78	1.73	1.674	11.86	33.3	0.806	0.917	13.8	16.39	15.8	−3.6
8	2.04	25.45	1.568	1.674	11.72	29.8	3.952	1.22	−69.1	14.51	16.4	13.0
9	2.04	25.40	1.435	1.628	11.68	26.5	3.981	1.63	−59.0	14.59	16.7	14.46
10	2.04	25.50	1.30	1.581	11.92	23.3	4.560	2.20	−51.8	15.00	16.9	12.66
11	2.04	25.45	1.159	1.628	11.92	19.3	5.340	3.36	−37.1	15.21	16.8	10.45
12	2.72	34.30	1.95	1.674	13.38	26.8	1.713	1.02	−40.4	20.34	23.4	15.04
13	2.72	34.22	1.795	1.674	13.40	24.2	2.957	1.31	−55.7	22.99	23.9	3.95
14	2.72	33.88	1.64	1.674	13.38	20.9	>5.420	2.05		<21.38	24.6	

[a] Test data source: Keeys et al. [20].
[b] Deviation $= (w_{\mathrm{lf,pre}} - w_{\mathrm{lf,exp}}) \times 100/w_{\mathrm{lf,exp}}$, $(w_{\mathrm{en,pre}} - w_{\mathrm{en,exp}}) \times 100/w_{\mathrm{en,exp}}$.

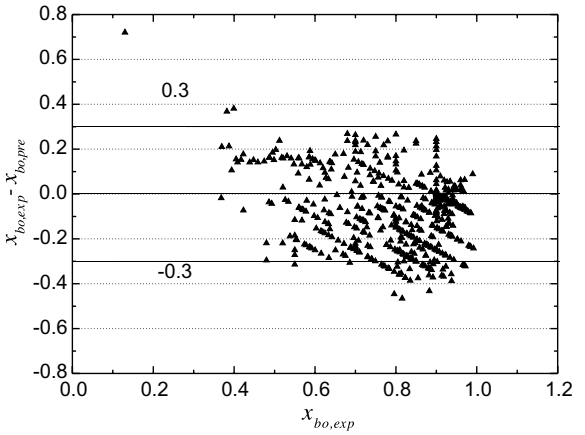

Fig. 2. Deviations of critical quality for steam–water flow in a vertical round tube.

4. Results and discussion

In this study, dryout data are measured in the horizontal tube. However, the present annular flow model is developed with vertical flow. Therefore, to compare the experimental results with the data predicted by the model, a correction factor for tube orientation must be considered. Wong et al. [22] suggested a correction factor for tube orientation, K_{hor}, as given in Eqs. (9) and (10), which are strongly dependent on the flow patterns. If mass flux is below G_{min}, full stratification would occur in a horizontal tube and consequently the CHF for horizontal flow becomes zero or $K_{\mathrm{hor}} = 0$. If mass flux is greater than G_{max}, the effects of tube orientation on CHF become negligible so that $\mathrm{CHF}_{\mathrm{hor}}$ can be assumed equal to $\mathrm{CHF}_{\mathrm{ver}}$.

$$\mathrm{CHF}_{\mathrm{hor}} = K_{\mathrm{hor}} \times \mathrm{CHF}_{\mathrm{ver}} \tag{9}$$

$$K_{\mathrm{hor}} = \left(\frac{G - G_{\mathrm{min}}}{G_{\mathrm{max}} - G_{\mathrm{min}}} \right)^{0.62} \tag{10}$$

In our experiments, the mass flux is greater than G_{max} for 95% of our total test runs. Therefore, the critical quality predicted by the present model is directly used in the comparison of the experimental data for a vertical tube by assuming $K_{\mathrm{hor}} = 1$.

Tables 2 and 3 show the measured and predicted critical qualities of this study, and also the data of Groeneveld et al.'s CHF table [23] in the 0.98 and 2.0 mm tube, respectively, which are determined based on equivalent steam–water conditions. Since dryout patches gradually enlarge in the liquid film, there physically exists quality range at which the temperature difference substantially varies. The range of x_{cr} in Tables 2 and 3 represents this quality range. Besides, the x_{cr} of the present model is evaluated based on

Table 2
Comparison of the measured with the predicted critical quality using the present model and Groeneveld et al.'s table [23] in 0.98 mm tube

Test run	Tube diameter (mm)	Evaporating temperature (°C)	Heat flux (kW/m^2)		Mass flux (kg/m^2 s)		Pressure (MPa)		Critical quality (%)		
			CO_2 (Exp.)	Steam–water (equivalent)	CO_2 (Exp.)	Steam–water (equivalent)	CO_2 (Exp.)	Steam–water (equivalent)	Groeneveld et al. [22]	Measured	Predicted
1	0.98	5	20	349.08	1000.0	1190.5	3.97	13.2	0.45–0.5	0.4–0.5	0.5–0.6
2			30	523.62					0.4–0.45	0.35–0.45	0.5–0.6
3			40	698.17					0.35–0.4	0.3–0.4	0.4–0.5
4			20	349.08	1500.0	1785.78			0.4–0.45	0.7–0.8	0.4–0.5
5			30	523.62					0.35–0.4	0.4–0.5	0.4–0.5
6			40	698.16					0.3–0.35	0.3–0.4	0.4–0.5
7			20	349.08	2000.0	2381.0			0.35–0.4	0.7–0.9	0.3–0.4
8			30	523.62					0.3–0.35	0.6–0.7	0.3–0.4
9			40	698.16					0.25–0.3	0.3–0.4	0.3–0.4
10		0	20	352.02	1500.0	1790.0	3.48	11.8	0.4–0.5	0.65–0.7	0.4–0.5
11			30	528.03					0.35–0.45	0.4–0.5	0.4–0.5
12		10	20	346.03			4.5	14.7	0.35–0.45	0.5–0.6	0.5–0.6
13			30	519.05					0.3–0.4	0.3–0.4	0.4–0.5

physical meaning of critical quality, which is represented by a range rather than an exact value.

As shown in Table 2, for the tube diameter of 0.98 mm, tests are conducted at saturation temperatures of 0, 5, and 10 °C, heat fluxes of 20, 30, and 40 kW/m^2, and mass fluxes of 1000, 1500, and 2000 kg/m^2 s. Fig. 3 compares critical qualities of the present tests with those of Hihara and Tanaka [4] as a function of critical heat flux and mass flux. In the present dryout data, increasing heat flux reduces the critical quality, but rather increasing mass flux slightly increases the critical quality. The test results of Hihara and Tanaka [4] and the data of Pettersen et al. [2] showed decreasing trends of critical quality with the rise of mass flux. Hihara and Tanaka [4] measured critical quality at mass fluxes of 360, 720, and 1440 kg/m^2 s, and Pettersen et al. [2] obtained the data when mass flux was below 1000 kg/m^2 s. These results may indicate that the slope of critical quality of CO_2 versus mass flux includes an inflection point when mass flux ranges from 1000 to 1500 kg/m^2 s.

As observed in the experimental data, critical quality and CHF become larger when mass flux increases beyond a specific limit that will be called transition mass flux in this paper. The transition mass flux varies as a function of saturation pressure. As mass flux increases beyond transition mass flux, more liquid droplet entrainment occurs. However, excessive liquid droplets in vapor core also increase liquid droplet deposition to liquid film layer and dryout patch regions. These trends improve the probabilities that dryout patches are rewetted and dryout of liquid film is prevented.

The transition mass flux of CO_2 is smaller than that of equivalent steam–water. The surface tension of equivalent steam–water is two times larger than that of CO_2. Because the contact angle of CO_2, as defined in Eq. (11) is smaller than that of the equivalent steam–water, the wettablity of CO_2 is larger than that of the equivalent steam–water. Large wettablity means that the possibility of dryout patches being rewetted will increase. Due to this smaller transition mass flux of CO_2, when mass flux is above transition mass flux, Groeneveld et al.'s table and the present model yield some deviations on the prediction of critical quality as compared to the present experimental data. Although the properties of CO_2 were successfully converted to that of equivalent steam–water properties, the effects of surface tension on deposition rate and wetting capability of dryout patch regions were not fully considered at high mass flux conditions in the present model due to limited data for those parameters in literature.

$$\cos\theta = 2\left(\frac{\sigma_{sg,d}}{\sigma_{lg}}\right)^{1/2} - 1 \tag{11}$$

However, when mass flux is lower than transition mass flux, the critical qualities of the experiment are well

Table 3
Comparison of the measured with the predicted critical quality using the present model and Groeneveld et al.'s table [23] in 2.0 mm tube

Test run	Tube diameter (mm)	Evaporating temperature (°C)	Heat flux (kW/m^2)		Mass flux (kg/m^2 s)		Pressure (MPa)		Critical quality (%)		
			CO_2 (Exp.)	Steam–water (equivalent)	CO_2 (Exp.)	Steam–water (equivalent)	CO_2 (Exp.)	Steam–water (equivalent)	Groeneveld et al. [22]	Measured	Predicted
1	2.0	5	7.9	97.25	500	595.26	3.97	13.2	X[a]	0.8	0.8–0.9
2			26	320.89					0.6–0.7	0.4–0.6	0.7–0.8
3			15.9	196.4	1000	1190.0			0.6–0.7	0.5–0.6	0.7–0.8
4			26.5	327.1					0.45–0.5	0.3–0.4	0.7–0.8
5			36.0	444.3					0.4–0.45	0.3–0.4	0.6–0.7
6			16.22	200.2	1500.0	1786.0	3.97	13.2	0.5–0.6	X	0.7–0.8
7			26.0	320.9					0.4–0.45	0.4–0.5	0.5–0.6
8			36.0	444.31					0.35–0.4	0.4–0.5	0.5–0.6
9			24.53	302.7	2000.0	2381.0			0.4–0.45	X	0.6–0.7
10			31.65	390.6					0.3–0.35	0.35–0.45	0.5–0.6
11			37.08	457.6					0.3–0.35	0.3–0.4	0.5–0.6
12			24.53	302.8	2500.0	2976.0			0.35–0.4	X	0.6–0.7
13			48.14	594.1					0.25–0.3	X	0.6–0.7
14			17.5	215.9	3000.0	3571.0			0.6–0.7	X	0.6–0.7
15			47.4	584.9					0.3–0.35	X	0.5–0.6
16		10	18.4	225.48	500.0	595.3	4.5	14.7	0.7–0.8	0.4–0.6	0.6–0.7

[a] X indicates non-dryout case.

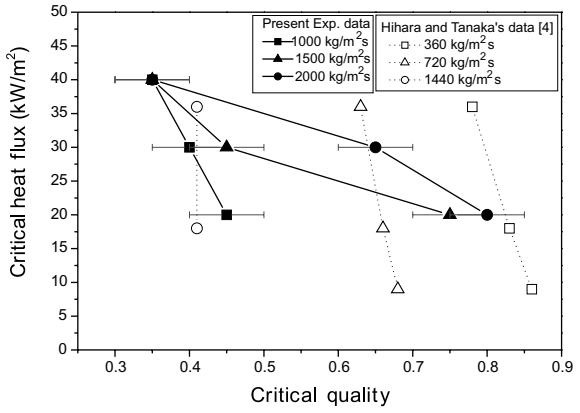

Fig. 3. Variations of critical quality with critical heat flux and mass flux.

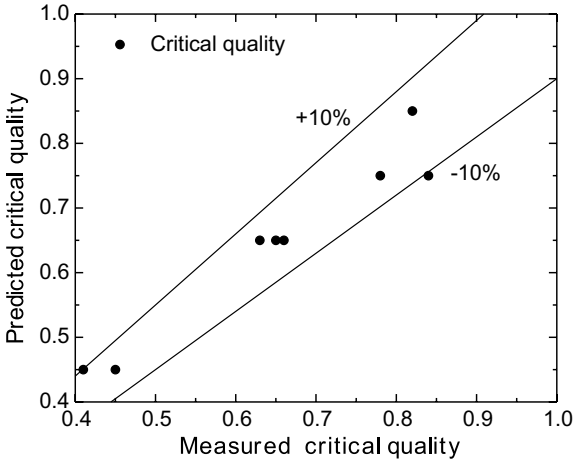

Fig. 4. Comparison of the predicted critical quality with the measured values for CO_2.

consistent with the predicted data using the present model. The average value of $|x_{bo,exp} - x_{bo,pre}|$ is 0.14 when the tube diameter is 0.98 mm. In addition, Fig. 4 shows the comparison of experiment data of Hihara and Tanaka [4] and the predicted dryout data of the present model. The predicted critical qualities show good agreement with the data of Hihara and Tanaka [4] within $\pm 10\%$ of the mean deviation.

For the tube diameter of 2.0 mm, as shown in Table 3, the experiment is conducted with more various heat fluxes and mass fluxes varying from 500 to 3000 kg/m^2 s with an interval of 500 kg/m^2 s. When mass flux is below 2500 kg/m^2 s, critical qualities are relatively well predicted from the present model and Groeneveld et al.'s table. When mass flux is 2500 and 3000 kg/m^2 s, dryout does not occur at any heat flux condition. Not only good wettability of CO_2, but also liquid droplet deposition prevents dryout patches from expanding at high mass flux conditions. The transition mass flux of CO_2 estimated from experimental data ranges from 2500 to 3000 kg/m^2 s. Although the present model shows better prediction than Groenveld et al.'s table, both models show poor estimation of critical quality as compared with the measured data at low heat flux and high mass flux conditions. However, the present model yields a relatively higher critical quality when dryout does not occur, which decreases the deviations of $|x_{bo,exp} - x_{bo,pre}|$.

As observed in Tables 2 and 3, the transition mass flux for the 2.0 mm tube is greater than that of the 0.98 mm tube due to a higher wettability of a smaller diameter tube. However, further studies are required to develop a generalized correlation for transition mass flux as a function of thermodynamic property, tube diameter, and saturation pressure. Besides, the accuracy of the present dryout model can be improved by investigating the relation between liquid droplet concentration in vapor core and the suppression of dryout patch extension under transition mass flux conditions.

5. Conclusion

The dryout phenomena of CO_2 are similar with those of steam–water in many respects. However, transition mass flux of CO_2 is smaller than that of steam–water because the wettability of CO_2 is larger than that of water. Higher wettability of CO_2 results from its lower surface tension. The critical quality during flow boiling of CO_2 is determined by using the analytical model based on the correlations for flow boiling of steam–water. In calculation of entrainment rate, two entrainment mechanisms of interface deformation and bubble bursting are used and critical liquid film thickness is successfully utilized to determine the occurrence of dryout. Dryout of CO_2 is well predicted with the present model before transition mass flux occurs. However, critical qualities are poorly predicted when mass flux is relatively high, at which deposition of liquid droplet is very active. Therefore, more extensive studies at high mass flux conditions need to be done for more precise dryout prediction considering low transition mass flux of CO_2.

Acknowledgements

This work was jointly supported by the Korea Science and Engineering Foundation (Grant no. 1999-1-304-006-3), the Korea University, and the Ministry of Commerce, Industry and Energy.

References

[1] J.S. Brown, Y. Kim, P.A. Domanski, Evaluation of carbon dioxide as R22 substitute for residential air conditioning, ASHRAE Trans. 108 (2) (2002).

[2] J. Pettersen, R. Rieberer, S.T. Munkejord, Heat transfer and pressure drop characteristics of evaporating carbon dioxide in microchannel tubes, in: Proceedings of 4th IIR-Gustav Lorentzen Conference, Purdue University, 2000, pp. 107–114.
[3] R. Yun, J.H. Hwang, Y.C. Kim, M.S. Kim, Evaporation heat transfer characteristics of carbon dioxide in a horizontal smooth tube, in: Proceedings of IIR Conference, Commission B1, Paderborn, Germany, 2001, pp. B2.15–B.21.
[4] E. Hihara, S. Tanaka, Boiling heat transfer of carbon dioxide in horizontal tubes, in: Proceedings of 4th IIR-Gustav Lorentzen Conference, Purdue University, 2000, pp. 279–284.
[5] P. Neksa, J. Pettersen, Heat transfer and pressure drop of evaporating CO_2 in microchannels and system design implications of critical heat flux conditions, in: ASME International Mechanical Engineering Conference and Exposition, New York, 2001, pp. 1–8.
[6] S.Y. Ahmad, Fluid to fluid modeling of critical heat flux: a compensated distortion model, Int. J. Heat Mass Transfer 16 (1973) 641–662.
[7] Y. Katto, H. Ohno, An improved version of the generalized correlation of critical heat flux for the forced convective boiling in uniformly heated vertical tubes, Int. J. Heat Mass Transfer 27 (9) (1984) 1641–1648.
[8] I.L. Pioro, D.C. Groeneveld, S.C. Cheng, S. Doeffer, A.Z. Vasic, Y.V. Antoshko, Comparison of CHF measurement in R-134a cooled tubes and the water CHF look-up table, Int. J. Heat Mass Transfer 44 (2001) 73–88.
[9] E.R. Holser, Flow patterns in high pressure two-phase (steam–water) flow with heat addition, Chem. Eng. Prog. Symp. Ser. 64 (82) (1968) 54–66.
[10] M. Ishii, K. Mishima, Droplet entrainment correlation in annular two-phase flow, Int. J. Heat Mass Transfer 32 (10) (1989) 1835–1846.
[11] T. Fujita, T. Ueda, Heat transfer to falling liquid films and film breakdown—I subcooled liquid film, Int. J. Heat Mass Transfer 21 (1978) 97–108.
[12] T. Fujita, T. Ueda, Heat transfer to falling liquid films and film breakdown—II saturated liquid films with nucleated boiling, Int. J. Heat Mass Transfer 21 (1978) 109–118.
[13] G.P. Celata, K. Mishima, G. Zummo, Critical heat flux prediction for saturated flow boiling of water in vertical tubes, Int. J. Heat Mass Transfer 44 (2001) 4323–4331.
[14] K.W. Lee, S.J. Baik, T.S. Ro, An utilization of liquid sublayer dryout mechanism in predicting critical heat flux under low pressure and low velocity conditions in rounds tubes, Nucl. Eng. Des. 200 (2000) 69–81.
[15] G..F. Hewitt, A.H. Goven, Phenomenological modeling of non-equilibrium flows with phase change, Int. J. Heat Mass Transfer 33 (2) (1990) 229–242.
[16] T. Saito, E.D. Hughes, M.W. Carbon, Multi-fluid modeling of annular two-phase flow, Nucl. Eng. Des. 50 (1978) 225–271.
[17] V.P. Carey, Liquid–Vapor Phase-Change Phenomena, Taylor & Francis, 1992, pp. 439–448.
[18] M. Ishii, M.A. Grolmes, Inception criteria for droplet entrainment in two-phase concurrent film flow, AIChE J. 21 (2) (1975) 308–326.
[19] T. Ueda, M. Inoue, S. Nagatome, Critical heat flux and droplet entrainment rate boiling of falling liquid films, Int. J. Heat Mass Transfer 24 (7) (1981) 1257–1266.
[20] R.K.F. Keeys, J.C. Ralph, D.N. Robets, The effects of heat flux on liquid entrainment in steam–water flow in a vertical tube at 1000 psia (6.894×10^6 N/m^2) AERE-R6294, U.K.A.E.A. Research Group, April 1970.
[21] K.M. Becker, G. Hernborg, M. Bode, O. Eriksson, Dryout data for flow of boiling water in vertical round ducts, annuli and rod clusters, AE-177, Heat Engineering Laboratory of AB Atom Energy, Sweden, March 1965.
[22] Y.L. Wong, D.C. Groeneveld, S.C. Cheng, CHF prediction for horizontal tubes, Int. J. Multiphase Flow 16 (1) (1990) 123–138.
[23] D.C. Groeneveld, L.K.H. Leung, P.L. Kirillov, V.P. Bobkov, I.P. Smogalev, V.N. Vinogradov, X.C. Huang, E. Royer, The 1995 look-up table for critical heat flux in tubes, Nucl. Eng. Des. 163 (1996) 1–23.